Desalination and Water Treatment
www.deswater.com
doi: 10.5004/dwt.2021.27474

231 (2021) 415–424
August

Conversion of eggshells to layered double hydroxides and their applications in Congo red removal

Songnan Li[a,*], Yuli Lu[b]

[a]*Modern Experimental Center, Harbin Normal University, Harbin, P.R. China 150025, Tel. +86 451 8806 0370; email: ok19841210@163.com*
[b]*Chengde Ecology Environmental Monitoring Center of Hebei Province, Chengde, P.R. China 067022, email: 44318580@qq.com*

Received 11 April 2021; Accepted 30 May 2021

ABSTRACT

In this study, calcined Ca-Al layered double hydroxides (CaAl-CLDHs) are synthesized from eggshells by adopting a facile and effective wet chemistry method, followed by calcination. A series of analysis methods such as X-ray diffraction, infrared, transmission electron microscopy are used for the detection of CaAl-CLDHs. The results show that the CaAl-CLDHs have the physical and chemical characteristics of layered double hydroxides. The CaAl-CLDHs were used to study the effect of the removal of Congo red. The influencing factors for Congo red removal, including dosage of CaAl-CLDHs and concentration of Congo red have been investigated, respectively. The better fit of the Langmuir model can be seen from the calculated data, by which the saturation adsorption capacity of the material for Congo red is derived as 840.3 mg/g. The pseudo-first-order, pseudo-second-order kinetic models were used to fit the experimental results. The pseudo-second-order kinetic model gives a satisfactory fit to all of the experimental data.

Keywords: Eggshells; Layered double hydroxide; Dye; Removal

1. Introduction

The absorption of dyes, by-product of textile and food industries, into water reservoirs is becoming a serious issue worldwide. The annual dye consumption is more than 10,000 and 100 tons of dyes are discharged into the water every year [1]. Water-containing dyes are hazardous for human health, and it threatens the environment as well. Therefore, the removal of dyes from water is of significant environmental importance [2]. Various techniques, such as electrocoagulation [3], flotation [4], chemical oxidation [5], filtration [6], membrane separation [7], photocatalytic [8,9], and adsorption [1], have been developed for removing dyes from wastewater. Among these methods, adsorption is an efficient, versatile, and convenient method. Variety of adsorption materials such as carbon material [10], molecular sieve [11], production waste [12], clay [13], polymer [14], and layered double hydroxide [15,16] has been investigated for adsorption of dyes from the aqueous solution [17,18].

Recently, the use of solid wastes instead of traditional adsorption materials to treat various kinds of wastewaters is more concerned [19–22]. Some biomass wastes can be used to prepare activated carbon, which can be used to remove pollutants. For example, Mittal et al. [23–26] prepared activated carbon materials from recycled wastes such as papaya peel and Curcuma and studied their ability to remove pollutants. However, the adsorption capacities of solid wastes are lower than traditional adsorption materials. To enhance the application value of solid wastes, many researchers focused on synthesizing a variety of effective adsorbents using solid wastes, such as industrial

* Corresponding author.

wastes and agricultural by-products, as precursors [27–29]. A lot of studies have established that the usage of nature-friendly solid wastes for water pollution control is an attractive and promising option with a double benefit for water treatment and waste management.

Layered double hydroxide (LDH) is a kind of functional material and has attracted wide attention because of its potential applications as adsorbents [30]. For instance, magnetic layered double hydroxide is used to remove dyes from aqueous solutions by Shan et al. [16]. Ahmed and Gasser [31] have synthesized of MgFe layered double hydroxides for removal of anionic reactive from wastewater, the results have shown, the saturated adsorption capacity of MgFe layered double hydroxides for Congo red was 105 mg/g. However, little research has been reported for the synthesis of layered double hydroxide from solid waste until now. Up to date, this material has been successfully synthesized from eggshells by ultrasound synthesis [32].

In this work, we reported the preparation of CaAl layered double hydroxides from eggshells by a facile wet chemistry method at room temperature. Congo red is found in printing, textile, and industrial wastewater and can be harmful to the human respiratory, digestive, and nervous systems. In this paper, it is used as a typical dye for adsorption [33]. The resulting products have excellent adsorption capability for removing Congo red. The influence of different experimental parameters, including CR concentration, the mass of CaAl-CLDHs, pH, and contact time, are determined to optimize the adsorption efficiency of CaAl-CLDHs to remove CR. Adsorption isotherms have been analyzed by Langmuir and Freundlich to clarify the adsorption process.

2. Materials and Preparation

2.1. Synthesis of Calcined Ca-LDHs

First, the collected eggshells were placed in a muffle furnace and calcined at 920° for 2 h. After that, 5 g of the above-calcined product was taken and dispersed into 50 mL of distilled water. The dispersion was stirred at room temperature and 50 mL of aluminum nitrate solution of a certain concentration was added to the above solution. The molar ratio of calcium to aluminum in the above-mixed solution is 4 to 1. After the reaction was continued for 2 h at room temperature, the precipitate was separated, washed, dried, and labeled as Ca-LDHs. CaAl-CLDHs were obtained by calcining Ca-LDHs at 450°C for 120 min.

2.2. Removal of Congo red

To multiple 150 mL conical flasks, 50 mL of Congo red solution was added, followed by the specified mass of the CaAl-CLDHs. These conical flasks were placed in a thermostatic shaker and run at 100 rpm under the specified conditions. The supernatant and adsorbent were separated at the end of the reaction and the concentration of Congo red in the supernatant was determined. The amount of the Congo red loading (mg) per unit mass of CaAl-CLDHs, q_e, and the % removal of Congo red were obtained by Eqs. (S1) and (S2), respectively.

2.3. Characterizations

The characterizations were seen in Supplementary Material.

3. Results and discussion

3.1. Characterization

The structure of the samples was investigated by XRD (seen in Fig. 1). The XRD patterns of the Ca-LDHs exhibited typical layered double hydroxides compounds, seen in Fig. 1a. All the peaks can be indexed according to the structures of layered double hydroxides [34, 35]. The $CaCO_3$ phase is observed at 2θ of 29.4° for all samples due to the dissolution of CO_2 and reaction with Ca^{2+}. Based on the results, it can be calculated that the basal spacing of the (003) plane in this work is 8.60 Å. This value is close to those reported in the literature for intercalation of NO_3^- ions in LDHs. For Ca-LDHs calcined at 500°C for 2 h, the diffraction peaks showed that LDHs structure is degenerated and converted to an amorphous material showed in Fig. 1b. After the removal of Congo red, the diffraction peaks of LDHs are recovered, which is known as the "memory effect", with slight shifts toward the high-angle side observed in Fig. 1c. It indicates that the basal spacing of CaAl-CLDHs after removal of Congo red (7.60 Å), which is lower than that of Ca-LDHs, is similar to the report for LDHs interlayered of OH^- due to the intercalation of OH^- ions in CaAl-CLDHs [15,36]. The morphological features of the Ca-LDHs are shown in Fig. 2. The as-prepared Ca-LDHs have a plate-like morphology with a size of 2–5 μm, and the smooth surface with sharp edges indicated the incomplete crystal growth process. IR spectra of the CaAl-LDHs, Congo red, and CaAl-CLDHs after adsorption are seen in Fig. 3. A broadband at 3,450 cm^{-1} and its angular deformation at 1,623 cm^{-1} appear in all spectra, which are attributed to the stretching vibration of the interlayered water and the OH groups. The sharp band with a peak central at 1,385 cm^{-1} is observed due to the stretching vibrations of nitrate

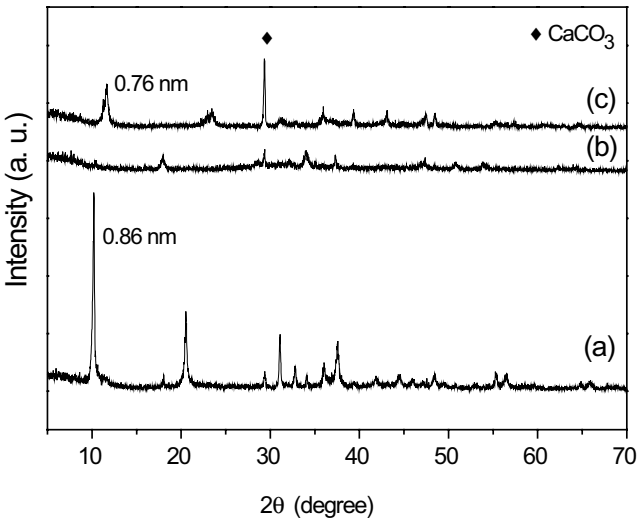

Fig. 1. Power XRD patterns of as-prepared CaAl-LDH (a), CaAl-CLDHs (b) and CaAl-CLDHs after removal of Congo red (c).

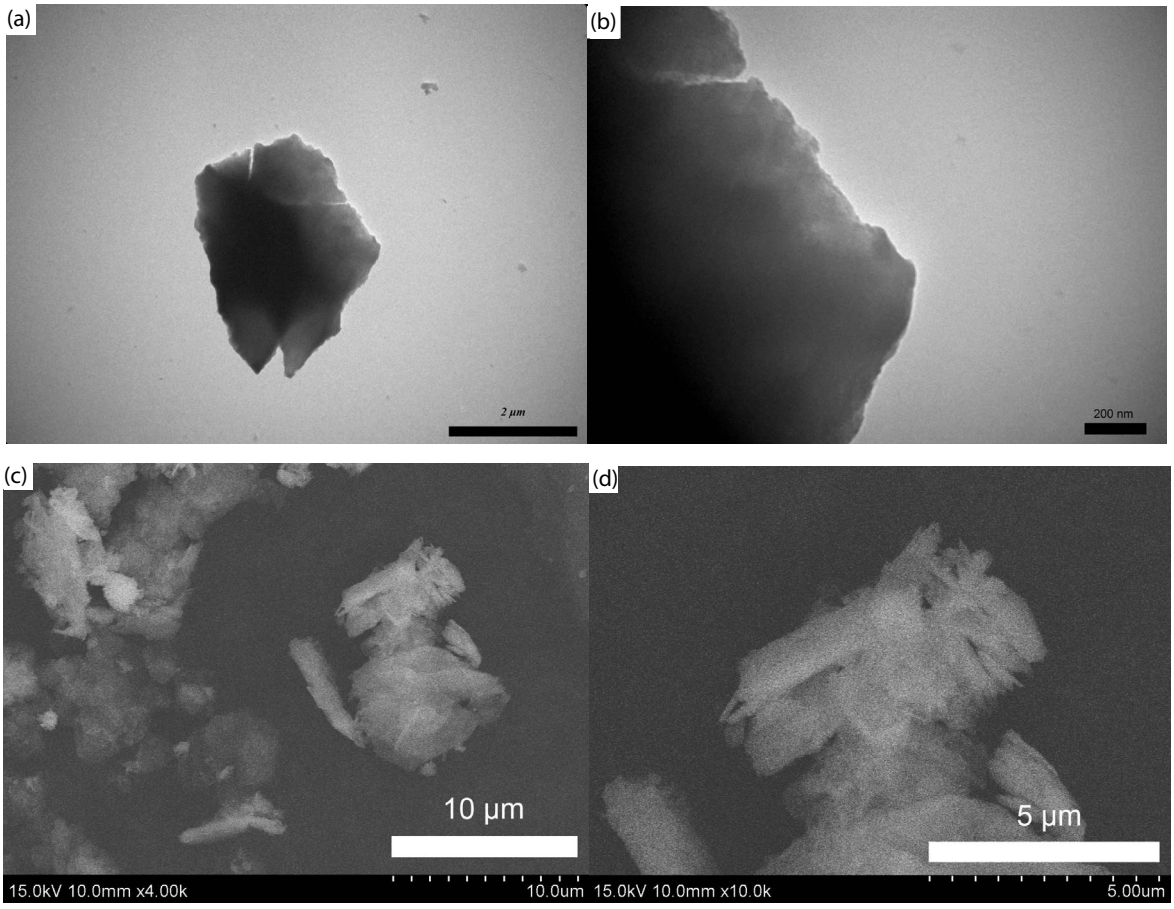

Fig. 2. TEM (a, b) and SEM (c, d) images of as-prepared CaAl-LDH.

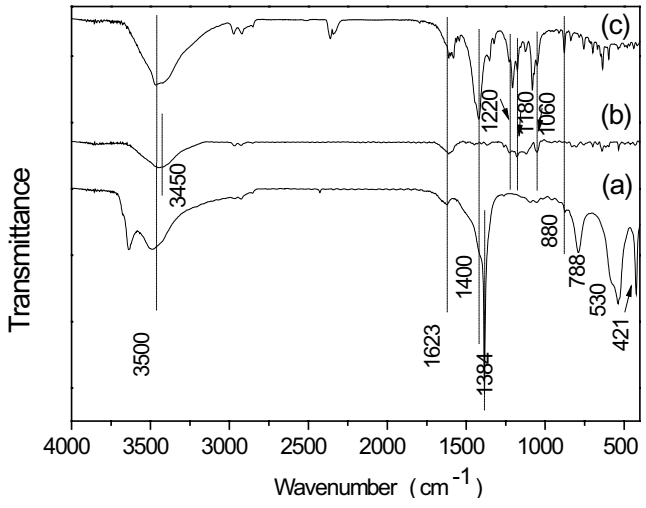

Fig. 3. FT-IR patterns of as-prepared CaAl-LDH (a), Congo red (b) and CaAl-CLDHs after removal of Congo red (c).

intercalated in the Ca-LDHs. In addition, because of the stretching vibration of CO_3^{2-} in $CaCO_3$, overlapping bands around 1,400 and 880 cm^{-1} are observed, consistent with the XRD pattern of $CaCO_3$ peak appear at 2θ of 29.4°. The vibrations of Me–O or Me–OH (Me = Calcium, Aluminum) occur less than 800 cm^{-1}. For the CR, the broad bands at 3,450 and 1,584 cm^{-1} are assigned to N–H and –N=N– stretching vibration, respectively. And, the bands at 1,060, 1,180 and 1,220 cm^{-1} are due to stretching of SO_3^{2-}. After adsorption of CR onto CaAl-CLDHs, the new bands were appeared in the range of 900–1,300 cm^{-1}, which can be associated with the characteristic absorption of CR, surmising the CR has been adsorbed onto the surface of CaAl-CLDHs. Notably, the shift of peaks for the sulfonate group shift to higher wavenumbers in the FTIR of CaAl-CLDHs after adsorption further confirms the electrostatic interaction between the Congo red and the surface of CaAl-CLDHs [16,31,37]. The thermal behavior of Ca-LDHs was investigated by TG-DTA. The Ca-LDHs exhibit mass losses in the temperature range 100°C–600°C can be seen in Fig. 4. Three regions of mass losses appear during this procedure. The first region rise to 140°C (DTA peak at 84°C) is due to the loss of adsorbed H_2O. The second region in the temperature range between 140°C and 400°C (DTA peak at 273°C) is due to the loss of the interlayer water and the hydroxyl group from brucite layers. The third region in the temperature ranges higher than 400°C is because of the loss of interlayer anions [38,39]. The nitrogen adsorption–desorption isotherms of as-prepared CaAl-LDH, CaAl-CLDHs, and CaAl-CLDHs after adsorption are investigated (seen in Fig. 5). All the products exhibit IV(a) isotherm and an H3(a)-type

hysteresis loop (P/P_0 = 0.4–0.99) according to the classification of IUPAC 2015, which are typical for mesoporous materials. The Ca-LDHs induce a specific surface area of 11.3 m^2/g. After calcination, the CaAl-CLDHs have a high specific surface area of 49.9 m^2/g due to the formation of pores by the expulsion of gas. After removing Congo red, the surface area decreased to about 5.7 m^2/g by recovering the original layered structure (seen in Table 1).

3.2. Effect of pH

The pH value is an indicator to characterize the adsorption performance. As shown in Fig. S1, the removal rate of Congo red was greater than 97% when the pH value of the solution was in the range of 6–9. The difference in the removal rate of Congo red in this range is not significant. Above or below this range has a negative effect on the removal rate of Congo red. It can be seen that the CaAl-CLDHs have a good removal effect on Congo red in this pH range. Therefore, the pH of the Congo red solution was not adjusted in the follow-up experiments.

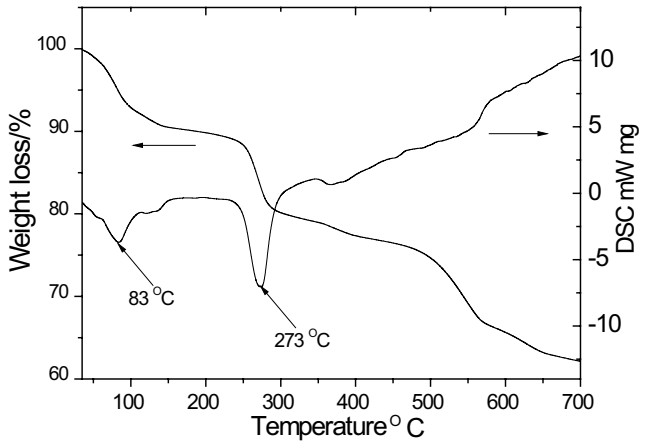

Fig. 4. TG-DTA curves of as-prepared Ca-LDHs.

3.2.1. Adsorbent dosage

The effect of the mass of CaAl-CLDHs on the Congo red removal was studied (Fig. 6). It can be seen from the graph that the removal rate of Congo red increases with the increase of CaAl-CLDHs mass. When the mass of CaAl-CLDHs is 0.05 g, the removal rate of Congo red approaches equilibrium (≥99%). This adsorbent dosage was also used in subsequent experiments.

3.2.2. Adsorption isotherms

The adsorption isotherms of Congo red on CaAl-CLDHs are shown in Fig. 7. And, the Langmuir isotherms (Eq. (4) in Supporting Information) and the Freundlich isotherms (Eq. (5) in Supporting Information) have been used to analyze the adsorption data. The adsorption isotherms are shown in Figs. 8 and 9. It was observed that the correlation coefficient for the Langmuir isotherm model (R^2 = 0.99) was higher compared to those for Freundlich (R^2 = 0.72) (Table 2). Therefore, Langmuir isotherm yielded a better fit to the experimental data with regard to Congo red adsorption on CaAl-CLDHs, which is consistent with the results of the nonlinear fit [40,41]. These facts suggest that Congo red was adsorbed in the form of monolayer

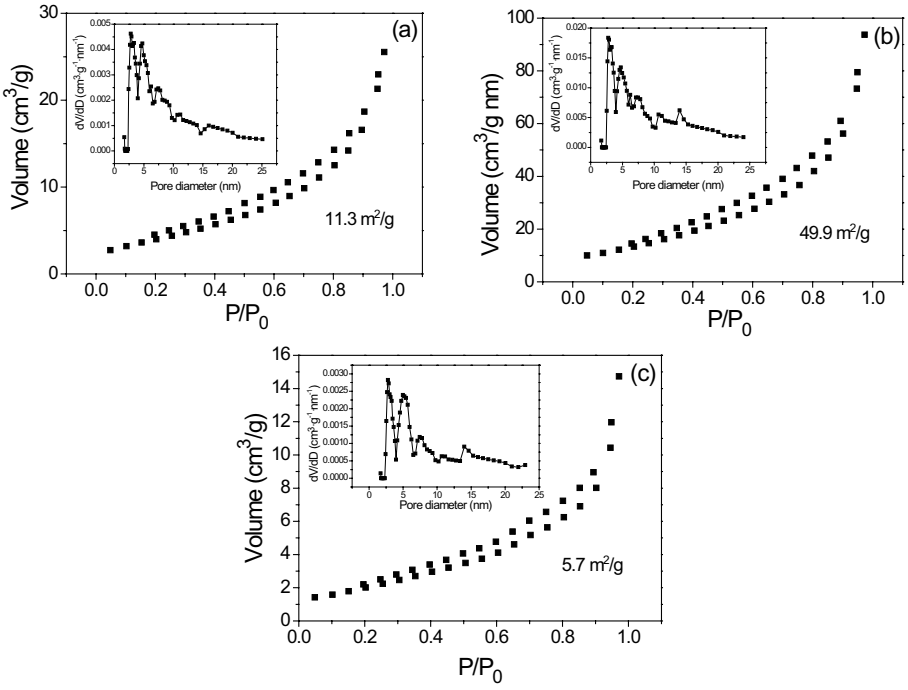

Fig. 5. N_2 adsorption-desorption isotherms and pore-size distribution (inset) of as-prepared CaAl-LDH (a), CaAl-CLDHs (b) and CaAl-CLDHs after removal of Congo red (c)

Table 1
Specific surface areas and pore parameters of different samples

Sample	Ca-LDHs	CaAl-CLDHs	CaAl-CLDHs after removal of CR
S_{BET} (m^2/g)[a]	11.3	49.9	5.7
V_P (cm^3/g)[b]	0.034	0.116	0.017
d_P (nm)[b]	2.77	2.76	2.77

[a]Performed by the multipoint BET method;
[b]Cumulative desorption pore volume and average pore diameter performed by the BJH method.

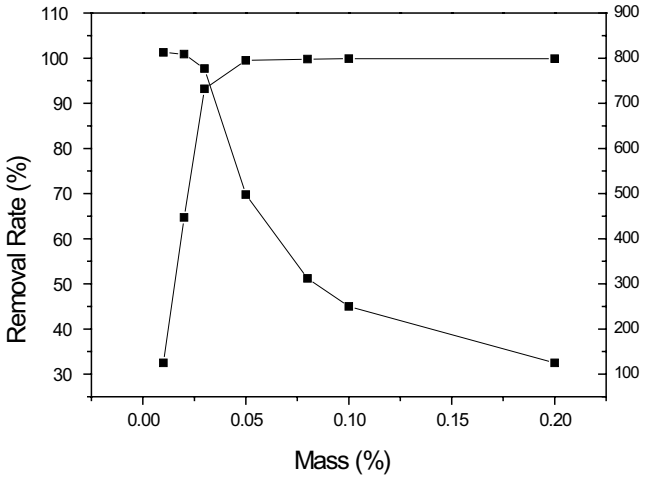

Fig. 6. Effect of solid/liquid ratio on adsorption of Congo red by CaAl-CLDHs. (Adsorption dosage 0.01–0.2 g, C_0 = 500 mg/L, retention time 2 h, T = 25°C and pH = 7).

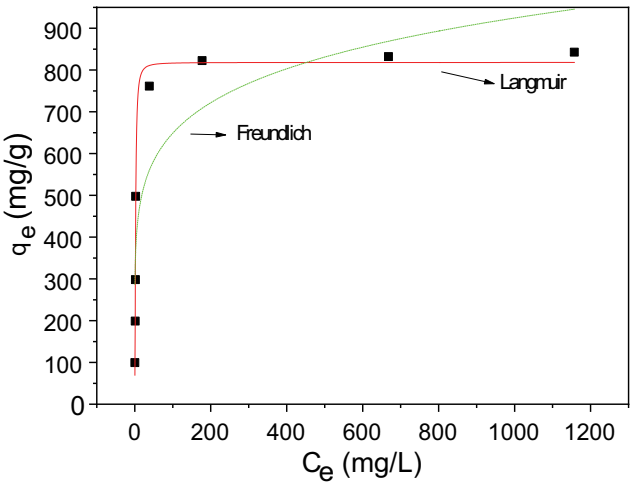

Fig. 7. Effect of Congo red concentration on the adsorption of Congo red by CaAl-CLDHs. (Adsorption dosage 0.05 g, C_0 = 100–2,000 mg/L, reaction time 2 h and pH = 7).

coverage on the surface of the adsorbent. The maximum adsorption capacity of the CaAl-CLDHs for CR can be calculated from the Langmuir isotherm to be 840.3 mg/g. The values of maximum adsorption capacity (q_0) and Langmuir

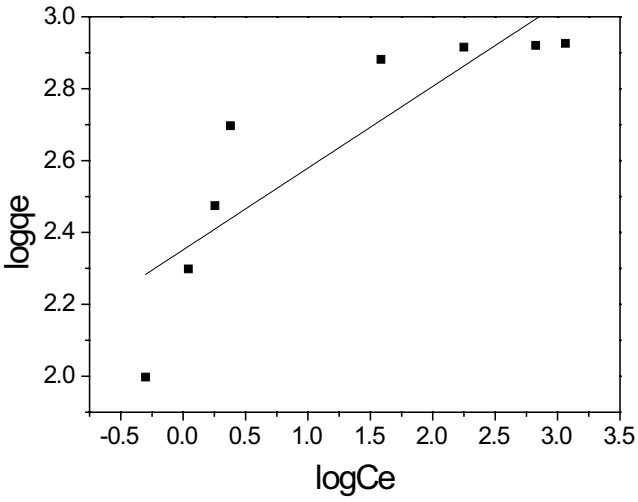

Fig. 8. Freundlich isotherm for removal of Congo red by CaAl-CLDHs.

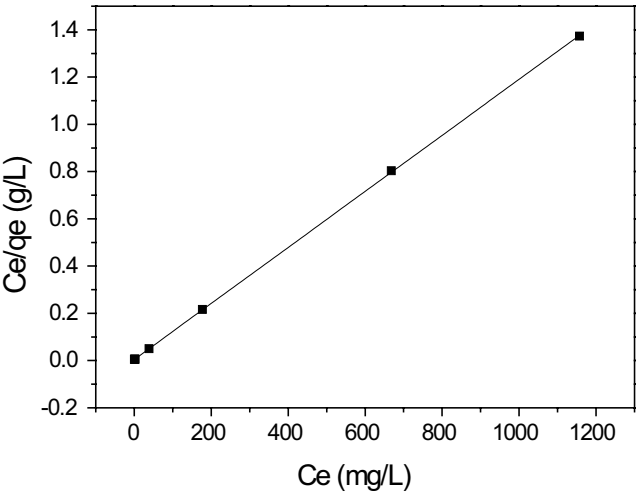

Fig. 9. Langmuir isotherm for removal of Congo red by CaAl-CLDHs.

constant (b) were evaluated from the intercept and slope of the Langmuir plots and given in Table 2. And, the values of K_f and n were obtained from the slope and intercept of the linear Freundlich plots and listed in Table 2. The calculated n lies in the range between 0.1 and 1, denoting favorable adsorption of Congo red onto the synthetic CaAl-CLDHs [42].

3.2.3. Adsorption thermodynamics

The adsorption studies were carried out at different temperatures 298, 308, and 318 K. The adsorption standard free energy ($\Delta G°$) was calculated from Eqs. (5)–(7) (Seen in Supporting Information) $\Delta H°$ and $\Delta S°$ are calculated from van't Hoff's equation and represented in Table 3, from the slope and intercept of the linear plot of ln$K$ vs. 1/T (Fig. 10). The standard enthalpy of adsorption $\Delta H°$= 14.95 kJ/mol indicated an endothermic process. The negative standard

Table 2
Isotherm parameters for adsorption of Congo red on CaAl-CLDHs

Freundlich			Langmuir		
k_F	n	R^2	q_e (mg/g)	b (L/mg)	R^2
224.84	0.2644	0.72	840.3	0.02644	0.999

Table 3
Thermodynamic parameters for adsorption of Congo red on CaAl-CLDHs

Temp. (°C)	$\Delta G°$ (kJ/mol)	$\Delta H°$ (kJ/mol)	$\Delta S°$ (J/mol/K)
25	–3.7793		
35	–4.4078	14.95	62.85
45	–5.0363		

free energy ($\Delta G°$) and the positive standard entropy ($\Delta S°$) indicate that the adsorption reaction is a spontaneous process and more favorable at higher temperatures [43,44].

3.3. Effect of adsorption time

At the conditions of 0.05 g CaAl-CLDHs, pH 7.0 and 100~1,000 mg L^{-1} Congo red, the time dependence of Congo red adsorption experiments are shown in Fig. 11. The result showed that the adsorption capacity of Congo red onto CaAl-CLDHs increases with the increase in adsorption time and reaches adsorption equilibrium within 2 h when the initial concentration of Congo red is 1,000 mg L^{-1}. And less time has been used to meet the adsorption equilibrium when the initial concentration of Congo red is lower than 1,000 mg L^{-1}. After 2 h, the change in adsorption capacity is not obvious.

3.3.1. Adsorption kinetics

To examine the diffusion mechanism, the experimental data are fitted to the pseudo-first-order (PFO) kinetic model and the pseudo-second-order (PSO) kinetic model, which is defined as Eqs. (8) and (9), respectively (Supporting Information). The result showed that the PSO kinetic model gives a satisfactory fit to all of the experimental data. The linear plots of Congo red adsorption kinetics to the PSO kinetic model and the calculated kinetic parameters are given in Figs. 12, 13 and Table 4, respectively. Based on $R^2 > 0.9999$, the adsorption kinetics is consistent with the PSO kinetic model. According to the hypothesis of this model, the adsorption of Congo red by CaAl-CLDHs is chemisorption. This result is corroborated by the non-linear fit. Electrostatic attraction and surface complexation are the two possible chemisorption mechanisms [45–47].

3.4. Effect of coexisting ions

As real-world wastewater is a multi-component system containing various organic and inorganic pollutants, it is important to study the effect of various

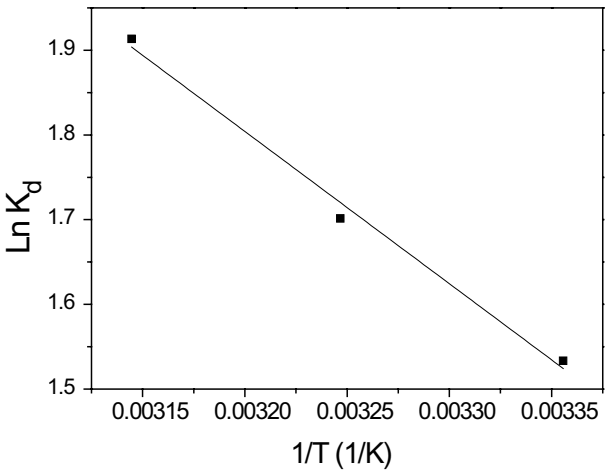

Fig. 10. Van't Hoff plot for removal of Congo red by CaAl-CLDHs.

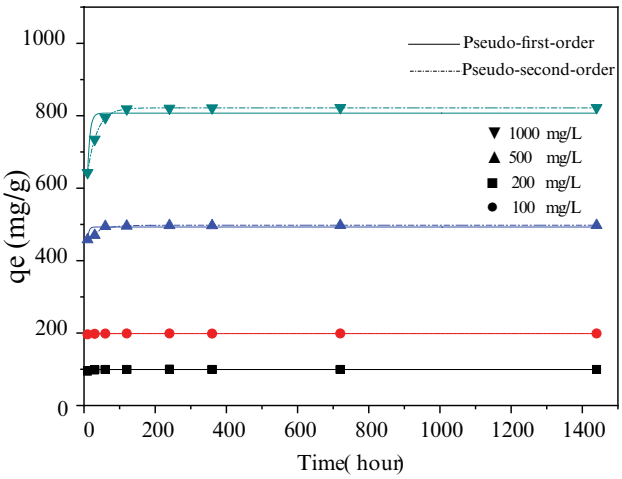

Fig. 11. Effect of reaction time on the adsorption of Congo red by CaAl-CLDHs.(Adsorption dosage 0.05 g, C_0 = 1,000 mg/L, reaction time 0.1 min-24 h, C_0 = 100–1,000 mg/L and pH = 6).

coexisting ions on the adsorption property. In this experiment, potassium salt was added as a coexisting anion, nitrate was added as a coexisting cation, and methylene blue was also added as a comparison. The concentrations of all the coexisting ions in solution were kept at 1 mmol/L. As shown in Fig. S2, the presence of cations has essentially no effect on the adsorption efficiency, and the presence of phosphate and carbonate causes some effect on the adsorption efficiency, which may be due to competitive adsorption. In addition, the presence of methylene blue also affected the adsorption effect.

3.5. Recyclability

The efficiency of recycling is an important parameter for adsorbents. In this study, the used CaAl-CLDH was calcined at 500°C and then used for adsorption of CR again. The results are shown in Fig. S3. It can be seen that the adsorption capacity of the adsorbent decreases more

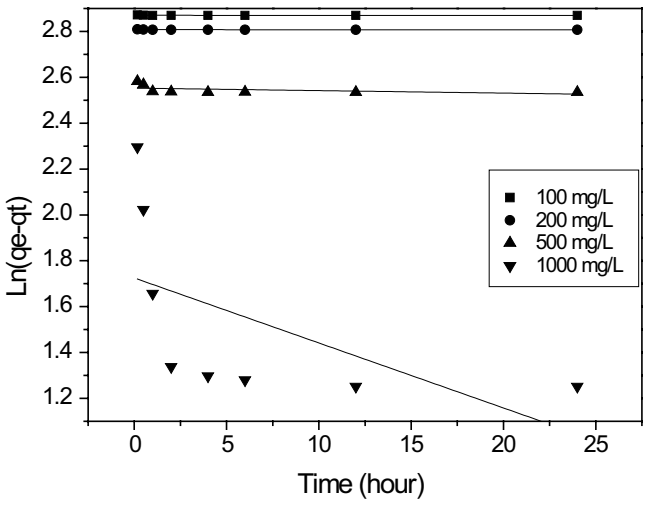

Fig. 12. Pseudo-first-order kinetics for removal of Congo red by CaAl-CLDHs.

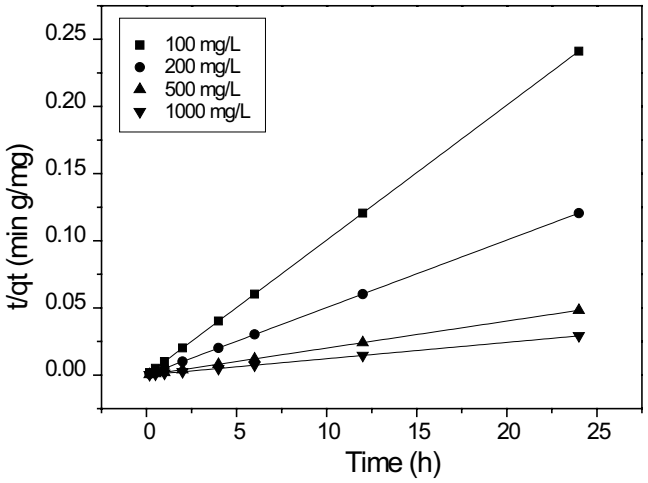

Fig. 13. Pseudo-second-order kinetics for removal of Congo red by CaAl-CLDHs.

significantly after the first recycling. The adsorption capacity of the adsorbent was slightly reduced for the subsequent cycles. Overall this adsorbent has a certain recycling capacity.

3.6. Comparison with other adsorbents

Table 5 depicts the adsorption capacities of different adsorbents for CR. It can be seen that the adsorption capacity of this material for CR is lower than that of hierarchical LDH synthesized by complex methods. However, it has advantages over other materials [48–52]. This indicates that this material has the prospect of practical application for dye removal in water.

4. Conclusion

Adsorbent CaAl-CLDHs are prepared by the wet chemistry method using eggshells as raw materials.

Table 4
Kinetic parameters for adsorption of Congo red on CaAl-CLDHs

Parameters	Co			
Concentration (mg/L)	100	200	400	1,000
Pseudo-first-order				
k_1 (min^{-1})	0.00036	0.00034	0.00109	0.28340
R^2	0	0.12	0.01	0.22
q_e (cal) (mg g^{-1})	11.1	10.5	8.5	4.2
Pseudo-second-order				
k_2 (g mg^{-1} min^{-1})	5.07	1.35	0.16	0.04
R^2	0.9999	0.9999	0.9999	0.9999
q_e (cal) (mg g^{-1})	99.5	199.2	397.5	826.4

Table 5
Comparison of performance of CaAl-CLDHs and other adsorbents with literature data

Adsorbent	Q_m (mg/g)	Reference
Hierarchical calcined Ni/Mg/Al-LDH	1,250	[48]
Hierarchical porous Ni/Co-LDH	909.2	[49]
NiAl-LDH	120.5	[50]
Powdered eggshell	95.25	[51]
Commercial CaO	238.66	[52]
Nano-CaO	357.14	[52]
Guar gum/activated carbon nanocomposite	831.82	[26]
CaAl-CLDHs	840.3	This work

The CaAl-CLDHs have excellent adsorption capacity for CR. Experimental data analysis indicates that the Langmuir adsorption isotherm indicates the adsorption of Congo red onto CaAl-CLDHs. The adsorption kinetic data indicate that the pseudo-second-order model is more appropriate for this result. The negative value of $\Delta G°$ at different temperatures indicates spontaneity and the positive value of $\Delta H°$ shows the endothermic nature of CR adsorption. The prepared CaAl-CLDHs have been demonstrated to be effective for removing CR with an equilibrium time of 2 h and optimal adsorption capacity of 840.3 mg/g.

Acknowledgements

This work was supported by the National Natural Science Foundation of China (21671050).

References

[1] M.T. Yagub, T.K. Sen, S. Afroze, Dye and its removal from aqueous solution by adsorption: a review, Adv. Colloid Interface, 209 (2014) 172–184.
[2] T.A. Nguyen, R.S. Juang, Treatment of waters and wastewaters containing sulfur dyes: a review, Chem. Eng. J., 219 (2013) 109–117.
[3] M.C. Wei, K.S. Wang, C.L. Huang, Improvement of textile dye removal by electrocoagulation with low-cost steel wool cathode reactor, Chem. Eng. J., 192 (2012) 37–44.

[4] K. Shakir, A.F. Elkafrawy, H.F. Ghoneimy, Removal of rhodamine B (a basic dye) and thoron (an acidic dye) from dilute aqueous solutions and wastewater simulants by ion flotation, Water Res., 44 (2010) 1449–1461.
[5] O. Türgay, G. Ersöz, S. Atalay, The treatment of azo dyes found in textile industry wastewater by anaerobic biological method and chemical oxidation, Sep. Purif. Technol., 79 (2011) 26–33.
[6] Y. Zheng, G. Yao, Q. Cheng, Positively charged thin-film composite hollow fiber nanofiltration membrane for the removal of cationic dyes through submerged filtration, Desalination, 328 (2013) 42–50.
[7] K.M.M. Nowak, Application of ceramic membranes for the separation of dye particles, Desalination, 254 (2010) 185–191.
[8] M. Solís, A. Solís, H.I. Pérez, Microbial decolouration of azo dyes: a review, Process Biochem., 47 (2012) 1723–1748.
[9] S. Zhou, G. Zhao, Y. Wang, L. Liu, F. Jiao, Fabrication of 3D multi-layered ZnCo-LDH as a heterogeneous photoactivator of peroxymonosulfate for efficient degradation of rhodamine B, Desal. Water Treat., 216 (2021) 315–325.
[10] V.K. Gupta, R. Kumar, N. Arunima, Adsorptive removal of dyes from aqueous solution onto carbon nanotubes: a review, Adv. Colloid Interface, 193–194 (2013) 24–34.
[11] S. Liu, Y. Ding, P. Li, Adsorption of the anionic dye Congo red from aqueous solution onto natural zeolites modified with N,N-dimethyl dehydroabietylamine oxide, Chem. Eng. J., 248 (2014) 135–144.
[12] M. Visa, A.M. Chelaru, Hydrothermally modified fly ash for heavy metals and dyes removal in advanced wastewater treatment, Appl. Surf. Sci., 303 (2014) 14–22.
[13] M.S. Rehman, M. Munir, M.Ashfaq, Adsorption of Brilliant Green dye from aqueous solution onto red clay, Chem. Eng. J., 228 (2013) 54–62.
[14] W.S. Ngah, L.C. Teong, M.A. Hanafiah, Adsorption of dyes and heavy metal ions by chitosan composites: a review, Carbohydr. Polym., 83 (2011) 1446–1456.
[15] H.Z. Boudiaf, M. Boutahala, L. Arab, Removal of methyl orange from aqueous solution by uncalcined and calcined MgNiAl layered double hydroxides (LDHs), Chem. Eng. J., 187 (2012) 142–149.
[16] R. Shan, L. Yan, K. Yang, Magnetic Fe_3O_4/MgAl-LDH composite for effective removal of three red dyes from aqueous solution, Chem. Eng. J., 252 (2014) 38–46.
[17] I. Anastopoulos, A. Mittal, M. Usman, J. Mittal, G. Yu, A.N. Delgado, M. Kornaros, A review on halloysite-based adsorbents to remove pollutants in water and wastewater, J. Mol. Liq., 269 (2018) 855–868.
[18] I. Anastopoulos, I. Pashalidis, A.G. Orfanos, I.D. Manariotis, T. Tatarchuk, L. Sellaoui, A.B. Petriciolet, A. Mittal, A.N. Delgado, Removal of caffeine, nicotine and amoxicillin from (waste)waters by various adsorbents. A review, J. Environ. Manage., 261 (2020) 110236.
[19] F. Deniz, S. Karaman, Removal of Basic Red 46 dye from aqueous solution by pine tree leaves, Chem. Eng. J., 170 (2011) 67–74.
[20] Y. Safa, H.N. Bhatti, Adsorptive removal of direct textile dyes by low cost agricultural waste: application of factorial design analysis, Chem. Eng. J., 167 (2011) 35–41.
[21] B.H. Hameed, R.R. Krishni, S.A. Sata, A novel agricultural waste adsorbent for the removal of cationic dye from aqueous solutions, J. Hazard. Mater., 162 (2009) 305–311.
[22] M. Ahmaruzzaman, Industrial wastes as low-cost potential adsorbents for the treatment of wastewater laden with heavy metals, Adv. Colloid Interface, 166 (2011) 36–59.
[23] H. Daraei, A. Mittal, Investigation of adsorption performance of activated carbon prepared from waste tire for the removal of methylene blue dye from wastewater, Desal. Water Treat., 90 (2017) 294–298.
[24] J. Mittal, R. Ahmad, A. Mariyam, V.K. Gupta, A. Mittal, Expeditious and enhanced sequestration of heavy metal ions from aqueous environment by papaya peel carbon: a green and low-cost adsorbent, Desal. Water Treat., 210 (2021) 365–376.
[25] C. Arora, P. Kumar, S. Soni, J. Mittal, A. Mittal, B. Singh, Efficient removal of malachite green dye from aqueous solution using *Curcuma caesia* based activated carbon, Desal. Water Treat., 195 (2020) 341–352.
[26] V.K. Gupta, S. Agarwal, R. Ahmad, A. Mirza, J. Mittal, Sequestration of toxic Congo red dye from aqueous solution using ecofriendly guar gum/activated carbon nanocomposite, Int. J. Biol. Macromol., 158 (2020) 1310–1318.
[27] D. Chen, C.Y. Mei, L.H. Yao, Flash fixation of heavy metals from two industrial wastes into ferrite by microwave hydrothermal co-treatment, J. Hazard. Mater., 192 (2011) 1675–1682.
[28] S. Bohra, D. Kundu, M.K. Naskar, One-pot synthesis of NaA and NaP zeolite powders using agro-waste material and other low cost organic-free precursors, Ceram. Int., 40 (2014) 1229–1234.
[29] A. Demirbas, Agricultural based activated carbons for the removal of dyes from aqueous solutions: a review, J. Hazard. Mater., 167 (2009) 1–9.
[30] D. Lv, Y. Wang, H. Li, GAC@Fe_3O_4, LDHs@Fe_3O_4 and GO@Fe_3O_4 applied to tetracycline hydrochloride removal in three-dimensional heterogeneous electro-Fenton process, Desal. Water Treat., 213 (2021) 328–834.
[31] I.M. Ahmed, M.S. Gasser, Adsorption study of anionic reactive dye from aqueous solution to Mg-Fe-CO_3 layered double hydroxide (LDH), Appl. Surf. Sci., 259 (2012) 650–656.
[32] S.N. Li, F.Y. Wang, X.Y. Jing, J. Wang, J. Saba, Q. Liu, L. Ge, D.L. Song, M.L. Zhang, Synthesis of layered double hydroxides from eggshells, Mater. Chem. Phys., 132 (2012) 39–43.
[33] J. Mittal, Permissible synthetic food dyes in India, Resonance, 25 (2020) 567–577.
[34] F.P. Sá, B.N. Cunha, L.M. Nunes, Effect of pH on the adsorption of Sunset Yellow FCF food dye into a layered double hydroxide (CaAl-LDH-NO_3), Chem. Eng. J., 215–216 (2013) 122–127.
[35] R. Rojas, Copper, lead and cadmium removal by Ca Al layered double hydroxides, Appl. Clay Sci., 87 (2014) 254–259.
[36] R.M. Santos, G.L. Gonçalves, V.R. Constantino, Removal of Acid Green 68:1 from aqueous solutions by calcined and uncalcined layered double hydroxides, Appl. Clay Sci., 80–81 (2013) 189–195.
[37] G. Zhang, L. Zhao, Synthesis of nickel hierarchical structures and evaluation on their magnetic properties and Congo red removal ability, Dalton Trans., 42 (2013) 3660–3666.
[38] S.L. Xu, Z.R. Chen, B.W. Zhang, J.H. Yu, F.Z. Zhang, D.G. Evans, Facile preparation of pure CaAl-layered double hydroxides and their application as a hardening accelerator in concrete, Chem. Eng. J., 155 (2009) 881–885.
[39] M.A. Woo, T.W. Kim, M.J. Paek, Phosphate-intercalated Ca-Fe-layered double hydroxides: crystal structure, bonding character, and release kinetics of phosphate, J. Solid State Chem., 184 (2011) 171–176.
[40] A. Mittal, R. Ahmad, I. Hasan, Biosorption of Pb^{2+}, Ni^{2+} and Cu^{2+} ions from aqueous solutions by L-cystein-modified montmorillonite-immobilized alginate nanocomposite, Desal. Water Treat., 57 (2015) 17790–17807.
[41] C. Arora, S. Soni, S. Sahu, J. Mittal, P. Kumar, P.K. Bajpai, Iron based metal organic framework for efficient removal of methylene blue dye from industrial waste, J. Mol. Liq., 284 (2019) 343–352.
[42] S. Soni, P.K. Bajpai, D. Bharti, J. Mittal, C. Arora, Removal of crystal violet from aqueous solution using iron based metal organic framework, Desal. Water Treat., 205 (2020) 386–399.
[43] K.L. Tan, B.H. Hameed, Insight into the adsorption kinetics models for the removal of contaminants from aqueous solutions, J. Taiwan Inst. Chem. Eng., 74 (2017) 25–48.
[44] K.Y. Foo, B.H. Hameed, Insights into the modeling of adsorption isotherm systems, Chem. Eng. J., 156 (2010) 2–10.
[45] E.C. Lima, A.A. Gomes, H.N. Tran, Comparison of the nonlinear and linear forms of the van't Hoff equation for calculation of adsorption thermodynamic parameters ($\Delta S°$ and $\Delta H°$), J. Mol. Liq., 311 (2020) 113315.
[46] M.I.E. Khaiary, G.F. Malash, Common data analysis errors in batch adsorption studies, Hydrometallurgy, 105 (2011) 314–320.
[47] H.N. Tran, S.J. You, A.H. Bandegharaei, H.P. Chao, Mistakes and inconsistencies regarding adsorption of contaminants

from aqueous solutions: a critical review, Water Res., 120 (2017) 88–116.
[48] C. Lei, X. Zhu, B. Zhu, C. Jiang, Y. Le, J. Yu, Superb adsorption capacity of hierarchical calcined Ni/Mg/Al layered double hydroxides for Congo red and Cr(VI) ions, J. Hazard. Mater., 321 (2017) 801–811.
[49] H. Hu, J. Liu, Z. Xu, L. Zhang, B. Cheng, W. Ho, Hierarchical porous Ni/Co-LDH hollow dodecahedron with excellent adsorption property for Congo red and Cr(VI) ions, Appl. Surf. Sci., 478 (2019) 981–990.
[50] D. Bharalia, R.C. Deka, Adsorptive removal of Congo red from aqueous solution by sonochemically synthesized NiAl layered double hydroxide, J. Environ. Chem. Eng., 5 (2017) 2056–2067.
[51] N. Yeddou, A. Bensmaili, Equilibrium and kinetic modelling of iron adsorption by eggshells in a batch system: effect of temperature, Desalination, 206 (2007) 127–134.
[52] H. Xia, L. Chen, Y. Fang, Highly efficient removal of Congo red from wastewater by Nano-Cao, Sep. Sci. Technol., 48 (2013) 2681–2687.

Supplementry information

S1. Characterizations

X-ray diffraction measurements used to characterize the crystalline phase were carried out on a Bruker D8 advance diffractometer, Fourier-transform infrared (FTIR) spectra were collected on a VERTEX80 spectrophotometer in the wavenumber range 400–4,000 cm^{-1}. Thermal analysis was performed by TG-DTA (EXSTAR 6300) under N_2. The Brunauer–Emmett–Teller (BET) specific surface areas of the products were analyzed by nitrogen adsorption in a NOVA 2000e nitrogen adsorption apparatus. All the products were degassed at 100°C prior to nitrogen adsorption measurements. The concentration of the Congo red was analyzed with a Cary4000 spectrophotometer, measuring the absorbance at λ_{max} = 488 nm.

S2. Formula

The amount of the Congo red loading (mg) per unit mass of CLDHs, q_e, and the % removal of Congo red were obtained by Eqs. (1) and (2), respectively:

$$q_e = \left(C_0 - C_e\right)\frac{V}{m} \tag{S1}$$

$$\text{Removal}\left(\%\right) = 100 \times \frac{C_0 - C_e}{C_0} \tag{S2}$$

where C_0 and C_e are initial and equilibrium concentrations in mg/L, m is the mass of adsorbent in grams, and V is the volume of solution in liters.

The adsorption isotherms thus obtained are depicted in Figs. 8 and 9.

The Langmuir and Freundlich equation has the form:

$$\frac{1}{q_e} = \frac{1}{q_0 b C_e} + \frac{1}{q_0} \tag{S3}$$

$$\log q_e = \log K_f + n \log C_e \tag{S4}$$

where C_e is the equilibrium concentration in the solution (mg/L), q_e is the amount adsorbed on the adsorbent at equilibrium (mg/g), q_0 is the maximum adsorption capacity (mg/g), b is a constant related to the adsorption energy (L/mg), K_f is the Freundlich adsorption constant (mg/g) $(L/mg)^n$, and n is the adsorption intensity parameter.

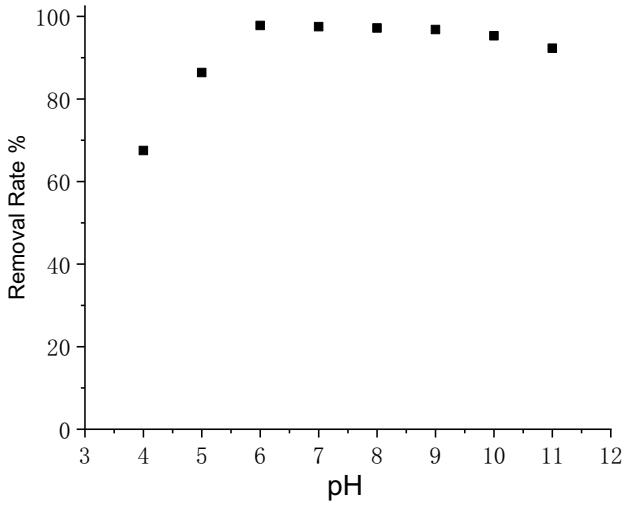

Fig. S1. Effect of solution pH on adsorption of Congo red by CaAl-CLDHs. (Adsorption dosage 0.05 g, C_0 = 500 mg/L, reaction time 2 h, T = 25°C and pH = 4–12).

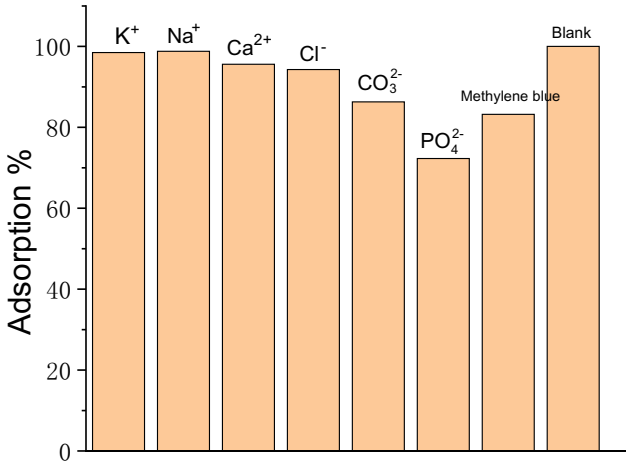

Fig. S2. Effect of the major cations and anions on adsorption.

The adsorption studies were carried out at different temperatures 298, 308, and 318 K. The adsorption standard free energy ($\Delta G°$) was calculated from

$$K = \frac{q_e}{C_e} \tag{S5}$$

$$\ln K = \frac{\Delta S°}{R} - \frac{\Delta H°}{RT} \tag{S6}$$

$$\Delta G° = \Delta H° - T\Delta S° \tag{S7}$$

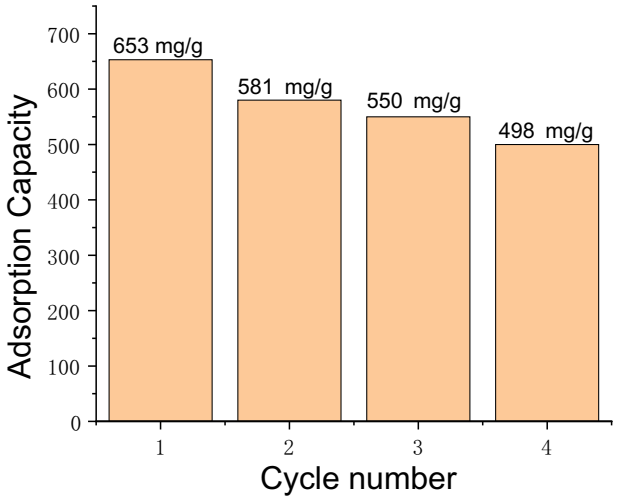

Fig. S3. Recyclability of CaAl-CLDHs for the CR adsorption.

where K is the Langmuir equilibrium constant; R is the gas constant (8.314 J/mol K) and T is the temperature in K. $\Delta H°$ and $\Delta S°$ are calculated from the van't Hoff's equation and represented in Table 3, from the slope and intercept of the linear plot of ln$K$ vs. 1/T.

In order to examine the diffusion mechanism involved during the adsorption process, various kinetic models were tested. Initially, the adsorption data are fitted to pseudo-first-order kinetic model, which is defined as:

$$\ln\left(q_e - q_t\right) = \ln q_e - k_1 t \tag{S8}$$

where q_e and q_t are the amount of Congo red adsorbed (mg/g) at equilibrium and at time t (min), respectively, and k_1 (min^{-1}) is the pseudo-first-order rate constant. Values of k_1 are calculated from the plots of ln(q_e – q_t) vs. t (Fig. 12) for the adsorbent samples. The R^2 values obtained are relatively small and the experimental q_e values do not agree with the values calculated from the linear plots.

Secondly, the pseudo-second-order kinetic model is expressed as the following:

$$\frac{t}{q_t} = \frac{1}{k_2 q_e^2} + \frac{t}{q_e} \tag{S9}$$

where q_e and q_t are the amount of Congo red adsorbed on adsorbent (mg/g) at equilibrium and at time t (h), respectively, and k_2 is the pseudo-second-order rate constant (g/mg h). Based on the experimental data of q_t and t, the equilibrium adsorption capacity (q_e) and the pseudo-second-order rate constant (k_2) can be determined from the slope and intercept of a plot of t/q_e vs. t.